A Ball-on-Beam Project Kit

by

Evencio A. Rosales

Submitted to the Department of Mechanical Engineering
In Partial Fulfillment of the Requirements for the
Degree of

Bachelor of Science in Mechanical Engineering
at the
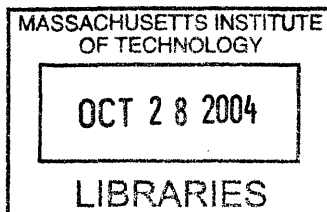Massachusetts Institute of Technology

June 2004

Signature of Author...
Department of Mechanical Engineering
May 7, 2004

Certified by...
David L. Trumper
Associate Professor of Mechanical Engineering
Thesis Supervisor

Accepted by...
Ernest G. Cravalho
Chairman, Undergraduate Thesis Committee

A Ball-on-Beam Project Kit

by

Evencio A. Rosales

Submitted to the Department of Mechanical Engineering
On May 7, 2004 in Partial Fulfillment of the
Requirements for the Degree of Bachelor of Science in
Mechanical Engineering

ABSTRACT

An apparatus of the classical ball-on-beam problem was designed and constructed to be used as a pedagogical instrument in feedback courses. The aesthetic and mechanical design incorporated economical materials to make kits of this apparatus attractive and cost effective. This thesis describes the design of the apparatus and the design of the two control loops to control the angle of the motor and the position of the ball along the beam. A lead compensator was used in each loop and an additional integrator was used in the motor loop to ensure the beam level when supporting the ball. The motor closed loop was designed for a bandwidth of 25 Hz and the ball loop was designed for 1 Hz. The closed loop control was implemented using a Matlab Simulink model and a dSPACE digital signal processor controller board. The feedback sensor of the motor angle was an encoder mounted to the back of the motor, and the sensor for the ball position was a linear potentiometer resistive element. After multiple iterations and debugging of the ball position sensor, the ball-on-beam system performed successfully, responding well to step commands and disturbances.

Thesis Supervisor: David L. Trumper
Title: Associate Professor of Mechanical Engineering

Table of Contents

List of Figures

List of Tables

Chapter 1: Introduction

This thesis describes the design and construction of a ball-on-beam balancing apparatus as well as the sensor and control design needed to balance a ball on a tilting beam. The kit of parts was given to students in an Electrical Engineering class on feedback systems as an end-of-term project.

1.1 Background

Balancing a ball on a tilting beam is a classic control problem. This application has been studied for years and methods of control techniques have been explained in the literature [1] - [5]. The task is to use an actuator to command a tilt angle on the beam and bring the ball, which rolls in one dimension along the beam, to a referenced position. First, the motor and beam must be controlled in an inner loop to a crossover frequency much higher than expected for the ball. Then, the outer loop is designed to compensate for the dynamics of the ball. Essentially, the controller must deal with two double integrators, the inertias of the ball and beam, and that of the ball.

1.2 Educational Functions

The ball-on-beam problem is a classic example of control theory that is studied by advanced undergraduate students. Because of its attention-grabbing nature, educational hardware companies such as Quanser® build models of the system [1], [2]. Demonstrations are commonly performed in classrooms by professors. Several configurations are available and some professors endeavor to craft their own design [3]. The industry standard for the ball position sensor is conductive plastic. Many of the experimental apparatus created by professors for classroom demonstration employ a more exotic ball position sensor such as an ultrasonic range transducer or photo diodes.

Because these apparatus are a good example of control theory, a course in feedback systems in the Electrical Engineering Department implemented the project as the final assignment for the class. Students received kits of the apparatus described in this thesis. The students were to create their own analog controller and make improvements to the plant and sensors. The remainder of this thesis will describe the procedure and reasoning for the kit, sensor selection, and control scheme implementation.

Chapter 2: Theoretical Model of the Plant

The underlying physics of the system must be understood before the hardware and controller are designed. By applying Newtonian mechanics, the forces and torques acting on the system can be shown and the dynamics understood.

2.1 Free Body Diagram

As seen in Figure 2.1, there are three main components that have moments and forces acting on them: the motor, the beam, and the ball. To simplify the derivation, the motor shaft and beam are considered to be a rigid body (i.e. the stiffness across the transmission is infinite), and centripetal acceleration is ignored. The pivot of the beam is also assumed to be near the plane of ball contact, and there is no skidding. To gather the equations of motion, sums of forces are calculated at points of interaction.
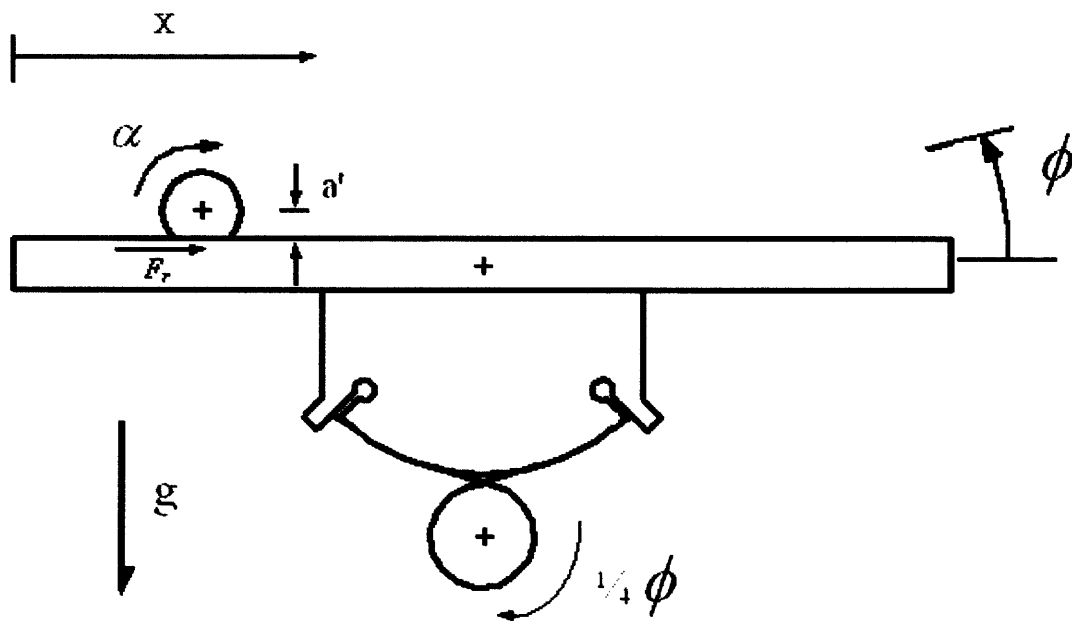
Figure 2.1. Free Body Diagram of Ball-on-Beam System. Infinite stiffness across the driving transmission is assumed.

Starting with the ball along the beam, the ball experiences a force due to the rolling constraint along the beam and a downward component due to gravity that depends on the angle, ϕ, of the beam. The sum of forces is as follows:

$$\Sigma F_b = mg \sin \phi - F_r = m\ddot{x}, \tag{2.1}$$

where the subscript b denotes forces acting on the ball, m is the mass of the ball, g is gravity, F_r is the rolling constraint force on the ball and x is the position of the ball along the beam. By geometry, the position can be defined as

$$x = \alpha \cdot a', \tag{2.2}$$

where α is the angular displacement of the ball, and a' is the distance between the axis of rotation of the ball and point of contact of the ball with the beam. The torque balance of the ball, τ_b, is also a product of the rolling constraint force as

$$\Sigma \tau_b = F_r a' = J_b \ddot{\alpha}, \tag{2.3}$$

where J_b is the moment of inertia of the ball,

$$J_b = \frac{2}{5} ma^2, \tag{2.4}$$

and a is the radius of the ball.

Next, the moment and force balances can be determined for the beam and motor. The beam bears the load of the ball as well as the input torque of the motor. The torque balance is given by

$$\Sigma \tau_{bm} = \tau_{in} = J_{bm} \ddot{\phi}, \tag{2.5}$$

where the subscript bm denotes the beam and motor, and τ_{in} represents the torque generated by the motor. Because the power amplifier acts as a current source, the motor is current driven and does not depend on voltage. The torque relation is

$$\tau_{in} = k_t I_{in}, \tag{2.6}$$

where k_t is the motor torque constant, and I_{in} is the current supplied to the motor.

Equations 1.1 through 1.6 constitute the primary equations of motion and geometric constraints. They can be combined and simplified to give the following equations:

$$\left(1 + \frac{2}{5}\left(\frac{a}{a'}\right)^2\right)\ddot{x} = g\sin\phi, \tag{2.7}$$

and

$$J_{bm}\ddot{\phi} = k_t I_{in}. \tag{2.8}$$

Because the system is expected to operate at or around a 0° beam angle, Equation 1.7 can be linearized using small angle approximations by

$$\left(1 + \frac{2}{5}\left(\frac{a}{a'}\right)^2\right)\ddot{x} = g\phi. \tag{2.9}$$

2.2 Transfer Functions

Equations 2.8 and 2.9 can be used to describe how one parameter dynamically relates to another. The most interesting transfer functions are from I_{in} to ϕ and from ϕ to x. The first will be used in the inner loop of the controller while the second will be used in the outer loop. Those transfer functions are given by

$$\frac{\phi(s)}{I_{in}(s)} = \frac{k_t}{J_{bm}s^2}, \tag{2.10}$$

and

$$\frac{x(s)}{\phi(s)} = \frac{g}{s^2\left(1 + \frac{2}{5}\left(\frac{a}{a'}\right)^2\right)}. \tag{2.11}$$

Overall, the uncontrolled system can be described from a current input to a ball position output by multiplying Equations 2.10 and 2.11. The fourth order system is given by

$$\frac{x(s)}{I_{in}(s)} = \frac{gk_t}{J_{bm}s^4\left(1 + \frac{2}{5}\left(\frac{a}{a'}\right)^2\right)}. \tag{2.12}$$

9

Chapter 3: Mechanical Design

The mechanical design was developed with the objective of implementing the kit as part of a lab project in Feedback Systems (6.302). The kits therefore had to be simple, cheap, and easy to assemble. In the design selected, the primary parts of the structure are the frame, transmission mechanism and balance beam (Figure 3.1). The transmission mechanism consists of a pulley on the motor shaft and a sector for gear reduction and smaller motor requirement. In addition to being a simplistic design, the figure is also sleek, stylish and decorative.
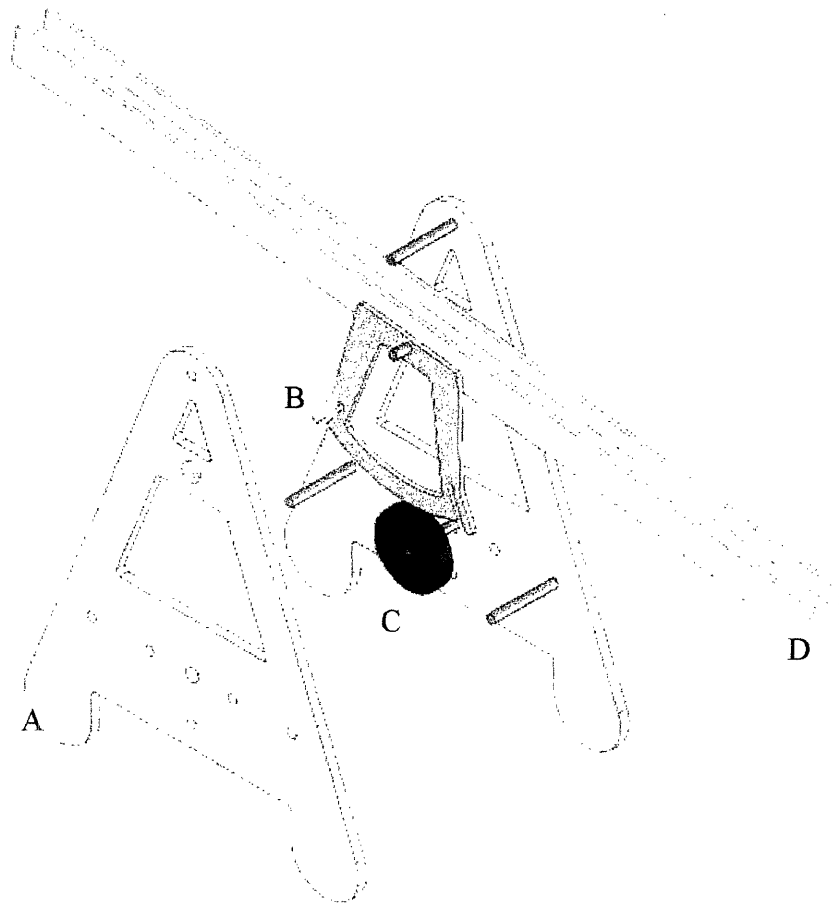

Figure 3.1. Solid Model of Apparatus. The primary parts of the structure are A) the Frame, B) the Sector, C) the Pulley, and D) the Beam.

3.1 Material Selection

To maintain low cost, materials were chosen for each specific component by considering durability, effectiveness, and cost. For the frame and sector, a low-cost polycarbonate was chosen. Polycarbonate is sufficiently stiff and lightweight compared to metal, and it resists corrosion and oxidation. The pulley on the motor shaft was made from stock Delrin, and the beam was made of basswood. The light weight and stiffness of basswood makes it a good choice to lower the moment of inertia while maintaining stiffness. Miscellaneous parts such as aluminum tubing and nylon bearings were used for bracing and assembling the apparatus. Table 3.1 shows a bill of materials per unit for a set of 50 kits. The total cost per kit is around $20, but does not include fabrication costs.

Material	Component	$/unit
Polycarbonate	Frame/sector	9.00
Delrin	Motor pulley	0.40
Bass wood	Beam	2.15
1/4" x 2-1/4" bolts	Bracing	0.60
3/8" Al tube	Bushing	0.33
1/4" Al tube	Beam shaft	0.10
1/4" Nylon bearing	Shaft bearing	0.52
Winchester Drive	DC motor	5.00
1" stainless steel ball	Ball	2.00
TOTAL:	**$20.10**	

Table 3.1. Bill of Materials. The materials used to produce 50 units of the ball-on-beam kit.

3.2 Manufacturing

Several manufacturing steps were taken to machine the raw materials. The construction was done using a lathe and a water jet cutter. Simple tools such a band saw and drill press were used to make minor cuts.

The first step in building the device was to cut the frame from a 1/4" polycarbonate sheet (Figure 3.2 a) and the sector from a 1/8" polycarbonate sheet (Figure 3.2 b). These pieces were cut in the water jet cutter for repeatability, relatively clean cuts, and speed. The tool paths for the parts were generated from a .dxf conversion of a SolidWorks solid model. A sector and two frames were cut in 15 minutes.
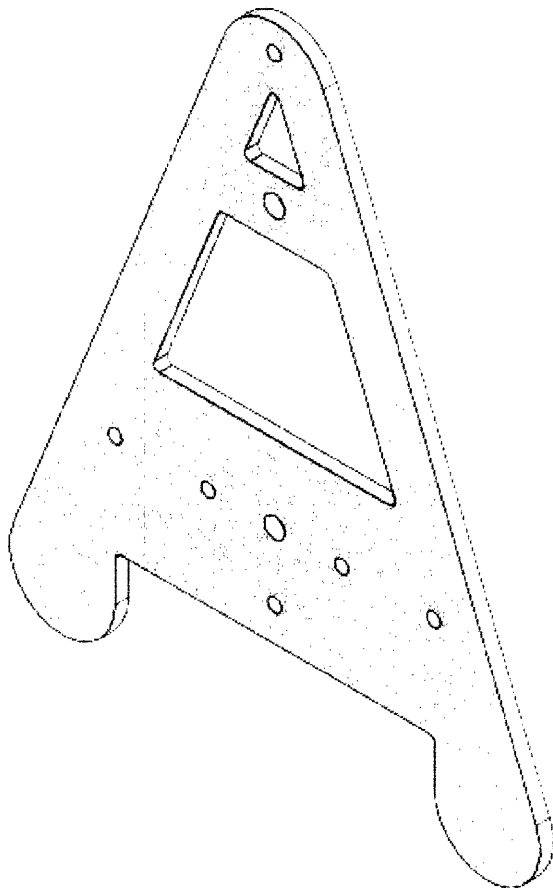
11

Figure 3.2a. Side frame made from polycarbonate. A part drawing is generated in SolidWorks and then machined in the water jet cutter.
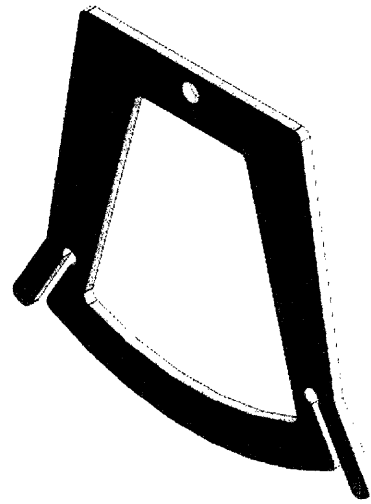
Figure 3.2b. Sector made from polycarbonate. Flexures provide preloading. Part drawing is generated in SolidWorks and part machined in water jet cutter.

The pulley that is attached to the motor shaft was made of 2" Delrin rod. A 3/8" section was cut from the stock and machined on the lathe. A 1/4" hole was drilled for the motor shaft, and a 1/16" deep groove was cut in the center of the circumference to guide the transmission belt. After using the lathe, a hole was drilled from the outside groove to the center hole to tap a setscrew.

Next, the beam was constructed using 2-foot-long basswood pieces. The dimensions of the model were decided by considering the proportion of beam center height and beam length. Because basswood is sold in 2-foot lengths, the beam was set at that length and the other dimensions were determined with respect to that adjustment. The pivot was placed 10 inches from the ground, and the overall height and width of the A-frame was set to 1 foot. The sector follows a designed developed by Stanford [6] with flexures for pre-tensioning the drive belt. The size of the sector was established by setting a gear ratio between the beam and motor of 4:1. Making the motor shaft pulley with a 1"

12

radius, the sector therefore had a 4" radius and an arbitrary 60° range. Once a beam that could support the conductive rail sensor was assembled, a 1/4" center hole was drilled, a 1/4" shaft was inserted, and the sector was attached.

Before final assembly, 2" bushings were cut from the 3/8" aluminum tube. At this point, the set-up was ready for assembly. The DC motor was fastened to the lower-middle portion of one of the frames, and the pulley was set on the motor shaft with a setscrew. Nylon bearings were then inserted into the guide holes for the beam shaft to rest. Next, the frames were put together with bolts, with the bushings separating them, the beam in between, and the motor outside the structure. The final step in assembly was to connect the pulley to the sector with a transmission belt. For this application, dental floss provided enough friction and tension. Figure 3.3 shows several fully assembled set-ups.
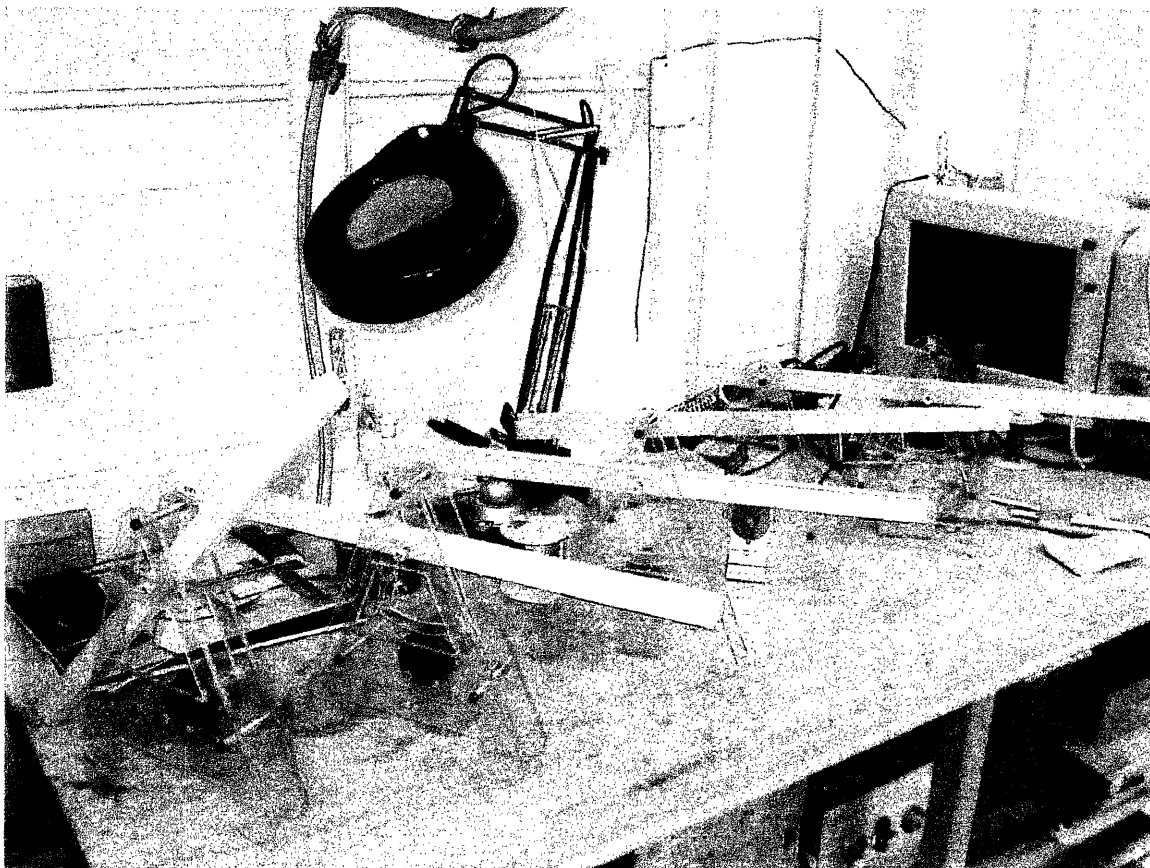

Figure 3.3. Fully Assembled Set-ups.

Chapter 4: Electronic Components

Substantial electrical work was necessary for the ball-balancer to function. The motor, angle sensor, ball position sensor, and power electronics needed wiring as well as tuning. The interface between the physical world and the digital world was a dSPACE controller board with a Com port connection to a computer. This board accepted inputs from the sensors and would output commands to the power amplifier, which in turn drove the motor. Figure 4.1 shows the equipment involved in powering the system and how the devices were connected.
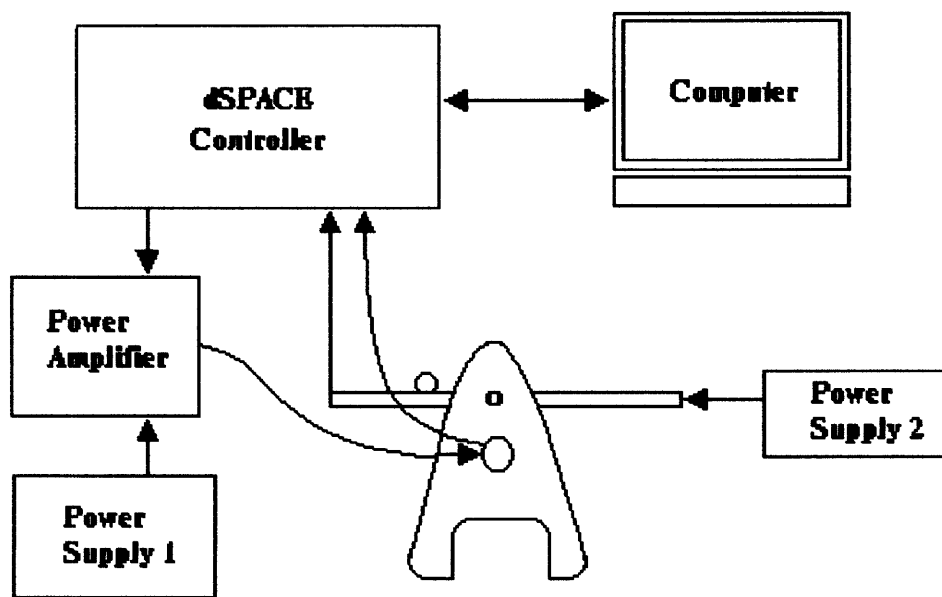
Figure 4.1 Schematic Diagram of Ball-on-Beam System. A dSPACE controller interfaced commands from a computer to output/input signals for the power amplifier and motion sensors of the ball balancer. Power supply 1 supplied power to the power amplifier while power supply 2 powered the ball position sensor.

4.1 DC Motor

The DC motor used in this application was a Winchester disk drive motor (Appendix A) that operates as a Lorenz force motor (Figure 4.2). As current, I, is driven through the outer coils in the direction of length l, a force, F_L, is applied orthogonal to the magnetic field, B, in the permanent magnets on the armature by the following law

$$\vec{F}_L = I \cdot \vec{l} \times \vec{B}. \tag{4.1}$$

By design of the armature, this force is always directed tangentially to the armature. It is by this perpendicular force that a torque, τ_m, is generated:

$$\tau_m = \vec{r} \times \vec{F}_L,$$ (4.2)

where r is the radius of the armature.
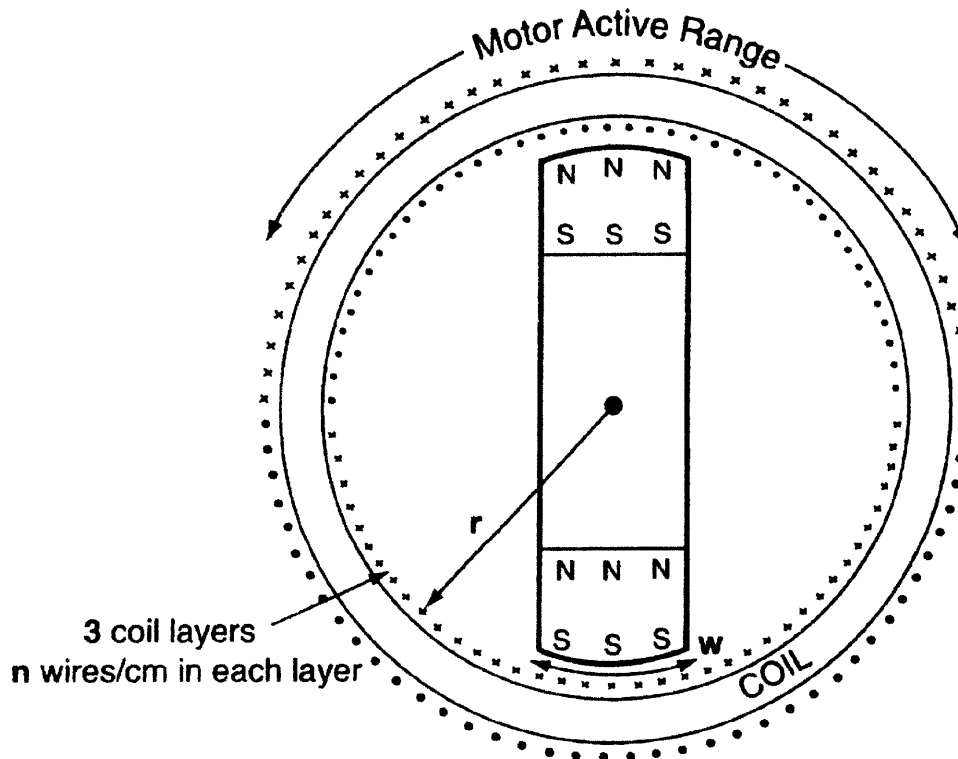
Figure 4.2. Diagram of DC Motor. A permanent magnet armature has a magnetic field that is perpendicular to the current running in the three layers of coils along the circumference of the motor. The coils reverse polarity midway, thus limiting the rotation of the motor shaft. Image taken from Mechatronics Lab Handout [7].

Because the coils reverse polarity to apply a force to both ends of the armature, the operating range is limited to about 115°. This can be viewed as a hindrance in most other applications, but because the beam is only expected to operate between ± 10°, this motor is sufficient even with a 4:1 gear ratio.

15

4.2 Angle Sensor

The angle sensor of the motor is an encoder mounted on the back of the Winchester drive. The sensor operates on the A/B quadrature method [8]. Two leads connected to the back of the motor case oscillate signal between ± 0.35 V in a sinusoidal mode as the shaft is turned. The two leads are out of phase by a quarter cycle (i.e. sin kθ and cos kθ), which gives a reference point. As the position of the shaft changes, so does the signal of the two leads, and when either signal changes sign a count is given, depending on if the sine is leading or lagging. The count is increased if the sine is lagging and decreased if the sine is leading. There are 1100 cycles in one rotation (k = 360°/1100), or 4400 counts per revolution. Therefore, the resolution of the encoder is 0.0818°. Figure 4.3 represents the concept of how A/B quadrature works.
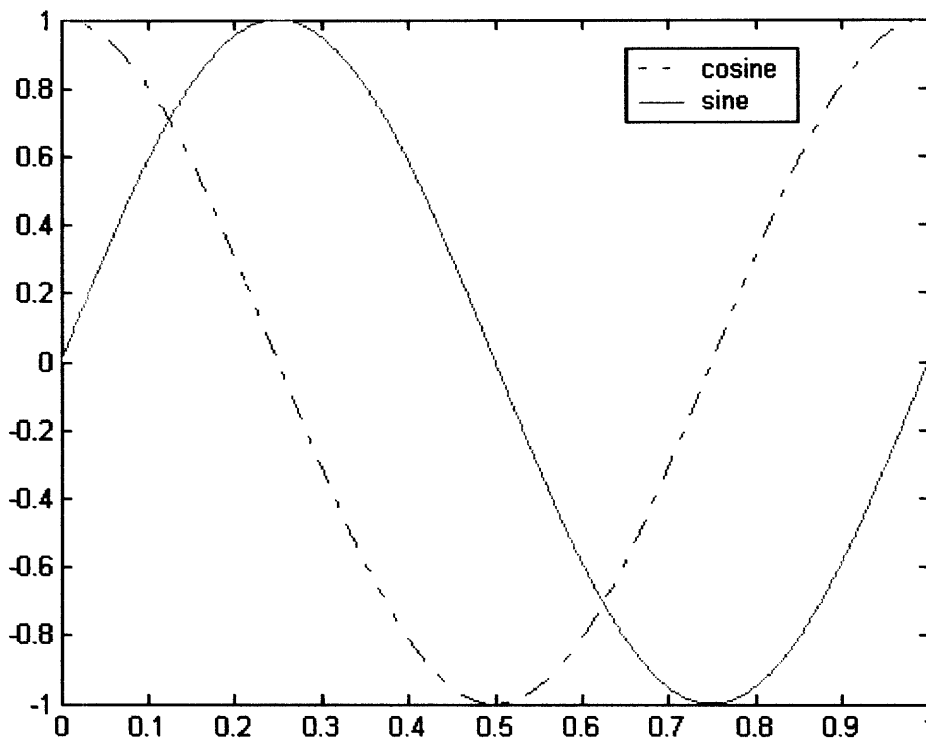
Figure 4.3. A/B Quadrature. Two signals, one sine (A), one cosine (B), vary as a function of angular position. As either of the two signals changes sign, a count is added or subtracted depending on if the cosine is leading or lagging the sine.

The encoder counts were summed by the encoder channel in the dSPACE board. Because dSPACE only distinguishes digital signals, an analog circuit (Figure 4.4) was constructed to digitize the sine and cosine signals and center them about 1.2 V. A 741 op-amp was used to supply a 1.2 V biased voltage and increase the amplitude of the signal to 1.2 V. A 74LS14 hex inverter with Schmitt trigger was used to relay an on/off signal at threshold voltages of 0.8 V and 1.6 V.

16

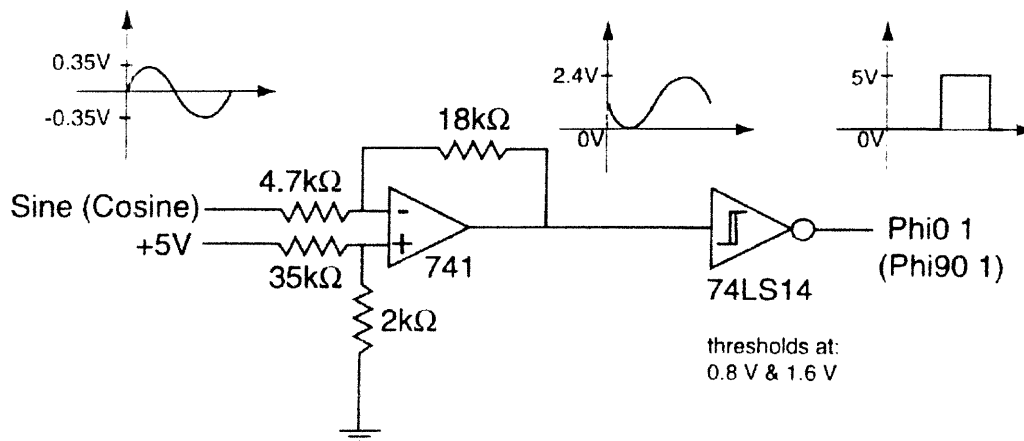Figure 4.4. Interface Circuit to Convert Encoder Signals. This circuit was used to convert the analog encoder sinusoidal signals into digital square waves with 2.4 V peak-to-peak amplitudes. Hysterisis induced by the Schmitt Trigger ensured that the signals surpassed a threshold voltage before assigning a count. Image taken from Mechatronics Lab Handout [7].

4.3 Ball Position Sensor

The ball position sensor used a linear potentiometer technique (Figure 4.5). Two resistive rails, one 5 V from end to end, and the other floating to be used as a probe, used a conductive steel ball as a wiper to transmit the voltage of the location of the ball, V_x, along the rail to the other rail. Here the voltage divider rule is used as follows:

$$V_x = V_{source} \frac{R_x}{R_t}, \tag{4.3}$$

where V_{source} is 5 V, R_t is the total resistance of the rail, and R_x is the resistance of the section of rail from ground to the point where the ball makes contact. By knowing at what voltage the ball is wiping a signal, the position of the ball can be correlated. This position calculation assumes that the resistances of the rails are linear, which by observation is true.
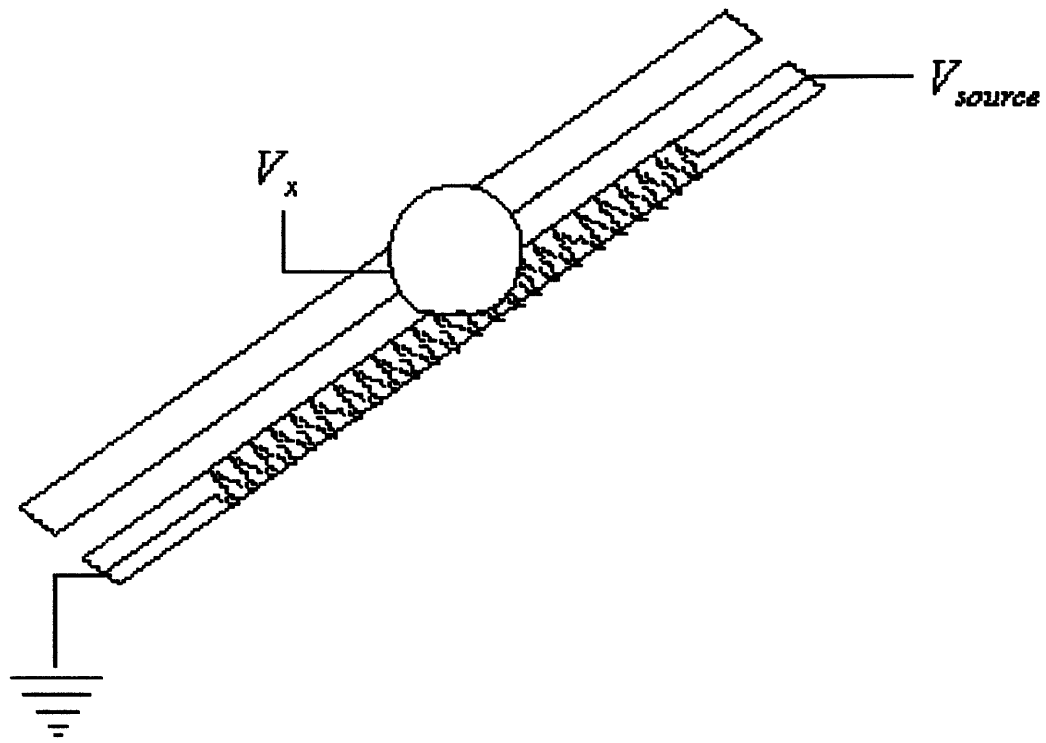
17

Figure 4.5. Linear Potentiometer Sensor. Two resistive rails were used to determine the position of the ball along the beam. One rail carried a 5 V potential from end to end, while the other rail used the ball as a wiper to measure the voltage correlating to the position of the ball.

Chapter 5: Control Design

The open-loop dynamics of the plant were discussed in Chapter 2. Equation 2.12 shows that the system is fourth order with four free integrators, which means the uncontrolled system is inherently unstable. To have the ball properly track a position command, a controller must be designed. The controller must be reliable and robust so as to not be easily excited into instability, and must also have good disturbance rejection. The disturbance rejection should compensate for the torque that the ball mass applies as it moves away from the center.

To begin, a block diagram for the closed loop system was constructed (Figure 5.1). In this system there are only two sensors available: the motor angle sensor and the ball position sensor. Therefore, there should be two closed loops, an inner motor loop and an outer ball position loop. Another intermediary loop sensing the beam angle would be beneficial in making the control and tuning of the system easier, but this loop is unnecessary and was not implemented in this project.
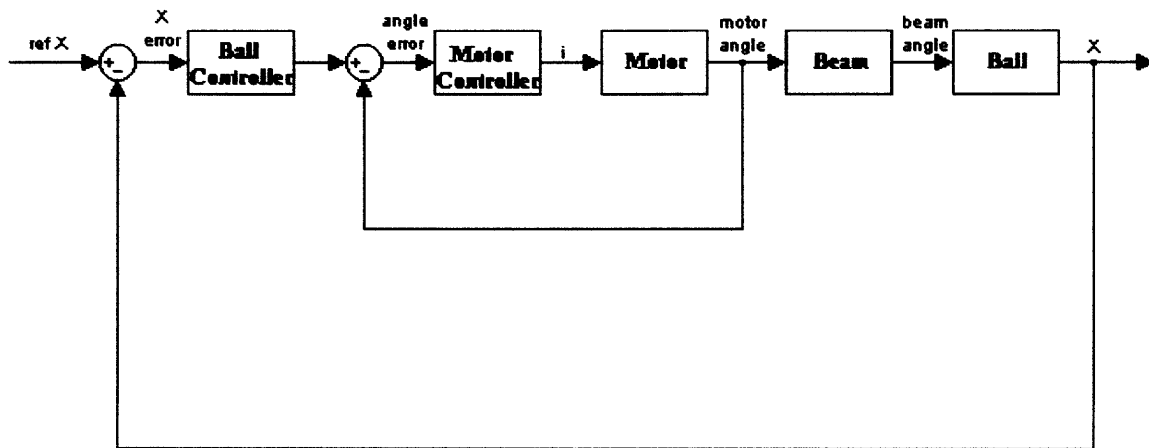
Figure 5.1. Block Diagram of Closed Loop Ball-on-Beam System. An inner loop controls the position of the motor, while the outer loop controls the position of the ball along the beam.

5.1 Motor Controller

The design parameters of the controller adhere to the realistic performance expectations of the system. For this application, a series of lead compensators were chosen to counteract the abundance of open loop poles and improve transient response. An integrator in the motor loop was also included to diminish the off-horizontal error of the beam and increase disturbance rejection. To make the motor loop effective to control the ball loop, the motor loop had to have a considerably higher bandwidth than the ball

position loop. Therefore, the realistic crossover frequency of the motor loop, ω_m, was arbitrarily chosen at about 25 Hz (158 rad/s). The lead compensator, G_{ml}, for the motor was thus designated as

$$G_{ml} = \frac{(s+50)}{(s+500)}.$$ (5.1)

In addition to the lead compensator, an integrator with a 0.5 s time constant was incorporated in cascade. The integrator transfer function,

$$G_{mi} = \frac{(0.5s+1)}{0.5s},$$ (5.2)

combined with the motor lead compensator became the motor controller,

$$G_{mc} = \frac{(0.5s+1)\ (s+50)}{0.5s(s+500)}.$$ (5.3)

The bode plots of the lead compensator, integrator, the complete motor controller and the open loop plant (Equation 2.10) are shown in Figure 5.2 and Figure 5.3. These plots show the open loop characteristics of the controller and plant. Once the controller and the motor are in cascade, the forward transmission transfer function for the motor becomes

$$G_{mol} = \frac{(0.5s+1)\ (s+50)k_t}{0.5s(s+500)Js^2}.$$ (5.4)
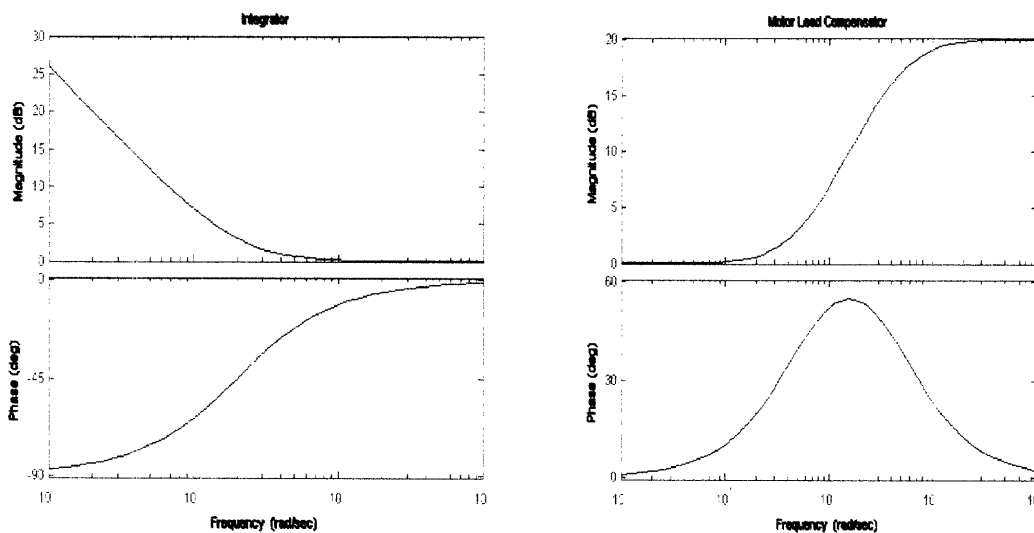
Figure 5.2. Model Bode Plots of Integrator and Lead Compensator.

20
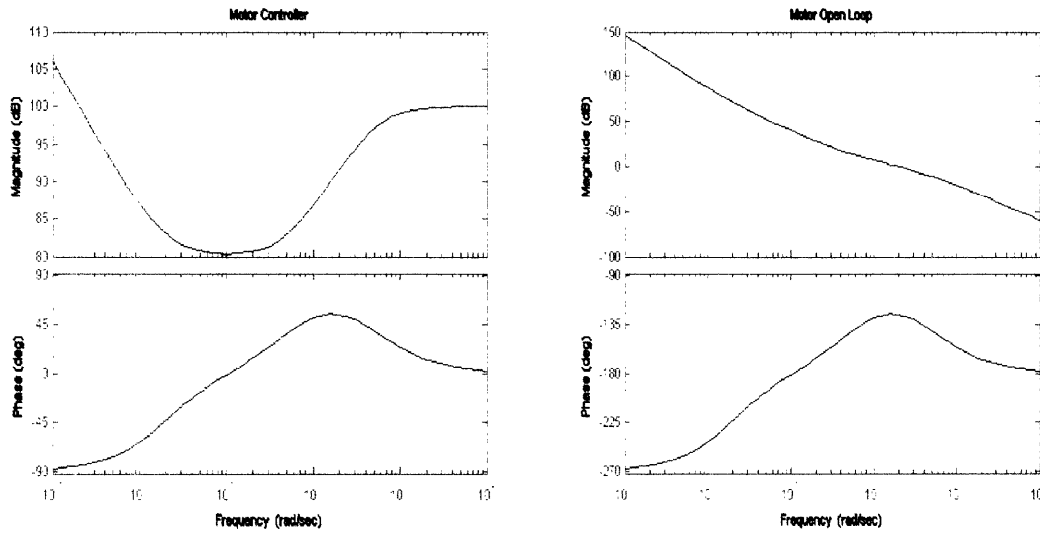
Figure 5.3. Model Bode Plots of Motor Controller and Motor Forward Loop.

Equation 5.4 can be manipulated using block diagram algebra to calculate the motor closed loop transfer function,

$$G_{mcl} = \frac{(0.5s+1)\ (s+50)k_t}{0.5s(s+500)Js^2 + (0.5s+1)\ (s+50)k_t}.$$

$$(5.5)$$

A step response of the motor closed loop transfer function is shown in Figure 5.4 and its corresponding Bode plot in Figure 5.5.

Figure 5.4. Theoretical Step Response of Closed Motor Loop.

Figure 5.5. Model Closed Motor Loop Bode Plot. With an integrator and a lead compensator, the motor loop became stable and had a gain of 0 at a bandwidth of 25 Hz.

5.2 Ball Controller

The transfer function in Equation 5.5 is the system that the ball controller acts upon. As can be inferred in Figure 5.5, with the inner closed loop, the system becomes much more manageable to control. Because the b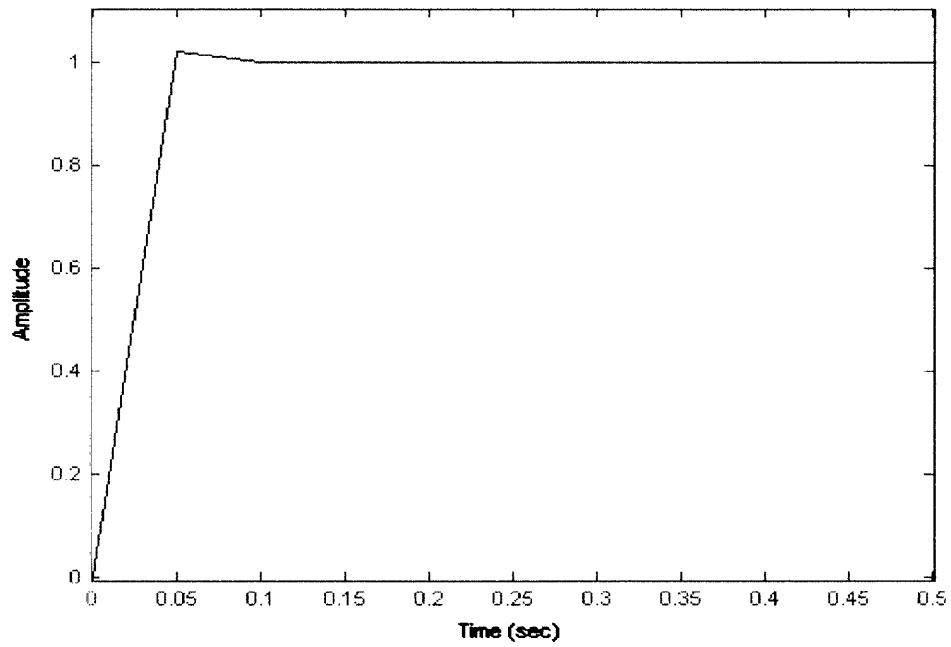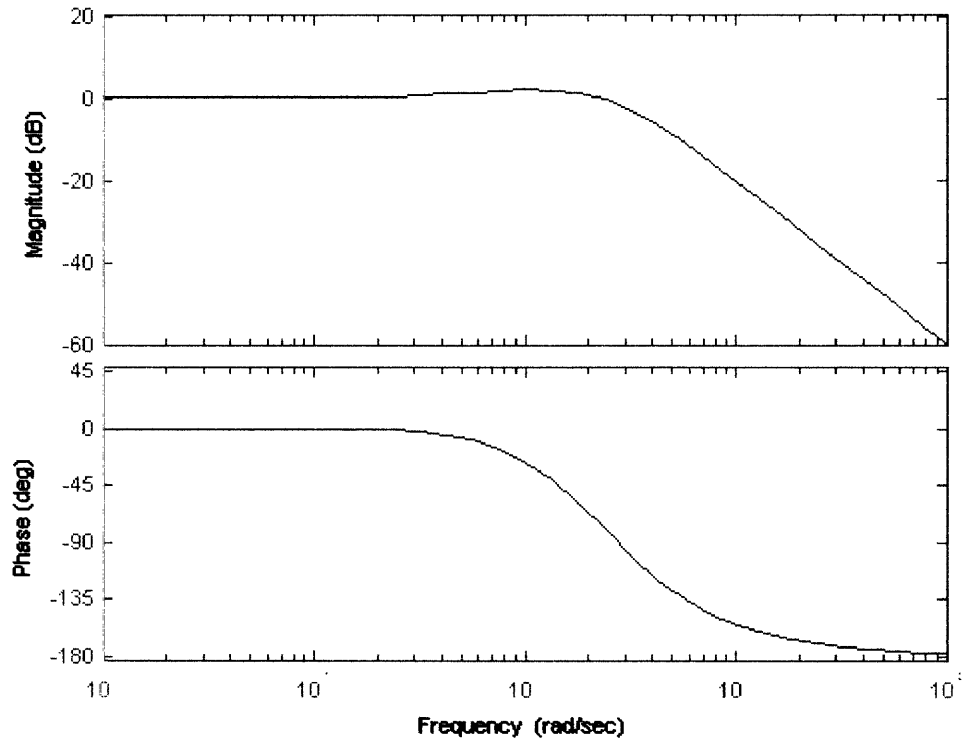andwidth of the ball-controlled system cannot realistically be near 25 Hz, the ball dynamics will not interfere with the motor dynamics. As was used in the motor loop, a lead compensator was implemented to control the ball position. A 1 Hz (6 rad/s) bandwidth was desired to be achieved with the following lead controller:

$$G_{bl} = \frac{(s+2)}{(s+20)}. \tag{5.6}$$

An integrator was not necessary in this loop because the integrator in the motor loop diminished the ball error as well. The ball controller combined with the closed motor loop gives the open loop transfer function of the ball position, G_{bol}:

$$G_{bol} = \frac{g(0.5s+1)\ (s+50)\ (s+2)k_t}{s^2\left(1+\frac{2}{5}\left(\frac{a}{a'}\right)^2\right)\left[0.5s(s+500)Js^2 + (0.5s+1)\ (s+50)k_t\right](s+20)}. \tag{5.7}$$

Figure 5.6 shows the Bode plot of the ball loop lead compensator and the forward path transmission, and Figure 5.7 shows the closed loop Bode plot of the ball position. The closed loop transfer function for the entire closed loop ball-on-beam system is

$$G_{sys} = \frac{g(0.5s+1)\ (s+50)\ (s+2)k_t}{s^2\left(1+\frac{2}{5}\left(\frac{a}{a'}\right)^2\right)\left[0.5s(s+500)Js^2 + (0.5s+1)\ (s+50)k_t\right](s+20) + g(0.5s+1)\ (s+50)\ (s+2)k_t}. \tag{5.8}$$
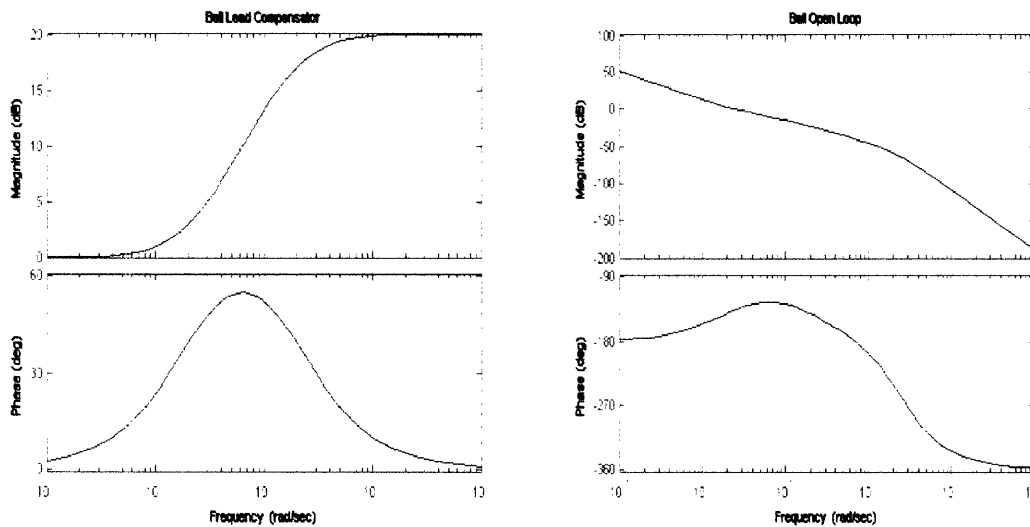
Figure 5.6. Model Bode Plots of Ball Controller and Forward Path Transmission.

23
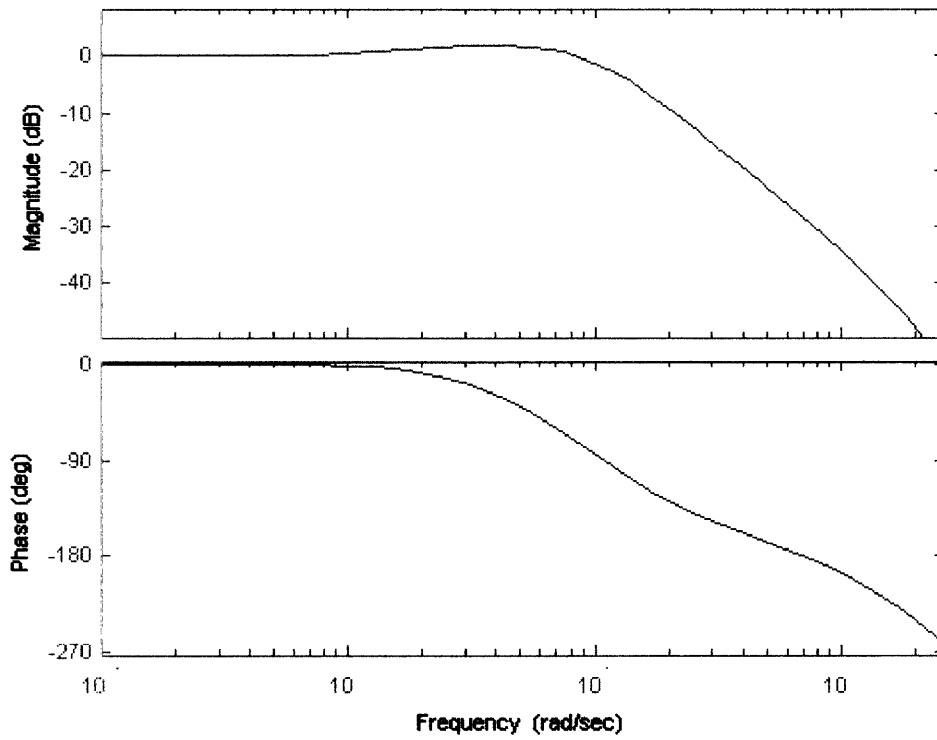
Figure5.7. Model Closed Loop Bode Plot of Ball Position.

5.3 Control Implementation

With dSPACE, the closed loop controls are implemented with a Simulink model (Figure 5.8). Blocks for each controller are arranged and the proper signals are routed from input to output to close the loop in computer space. These signals are then mapped and become variables in the graphical user interface, ControlDesk. Within this software, a control panel (Figure 5.9) can be designed using plotters, displays, slide bars, input boxes, etc., to view signals and vary parameters of the system.
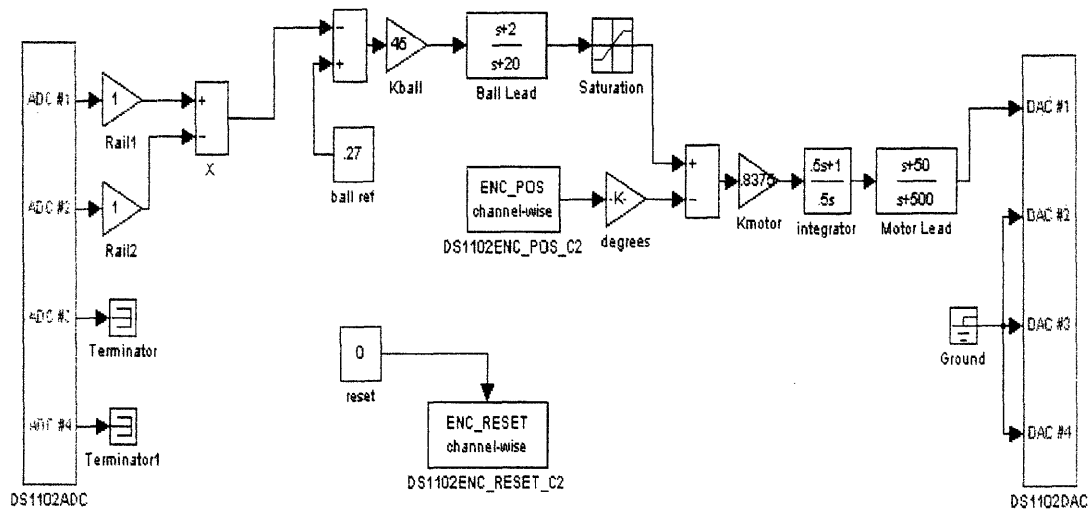
Figure 5.8. Simulink Model of Control Implementation. Blocks from the Simulink model library were used to construct the controllers and direct signals from input to output.

Figure 5.9. ControlDesk Control Panel. In this graphical user interface, numerical displays and plotters were used to view different signals while slider bars, and input boxes were used to adjust parameters of the control system.

Chapter 6: Test Results

A series of tests were conducted to verify the performance of the control design. Step responses and bode plots were measured for the motor angle, and ball position. Bode plots were measured dynamically using a Simul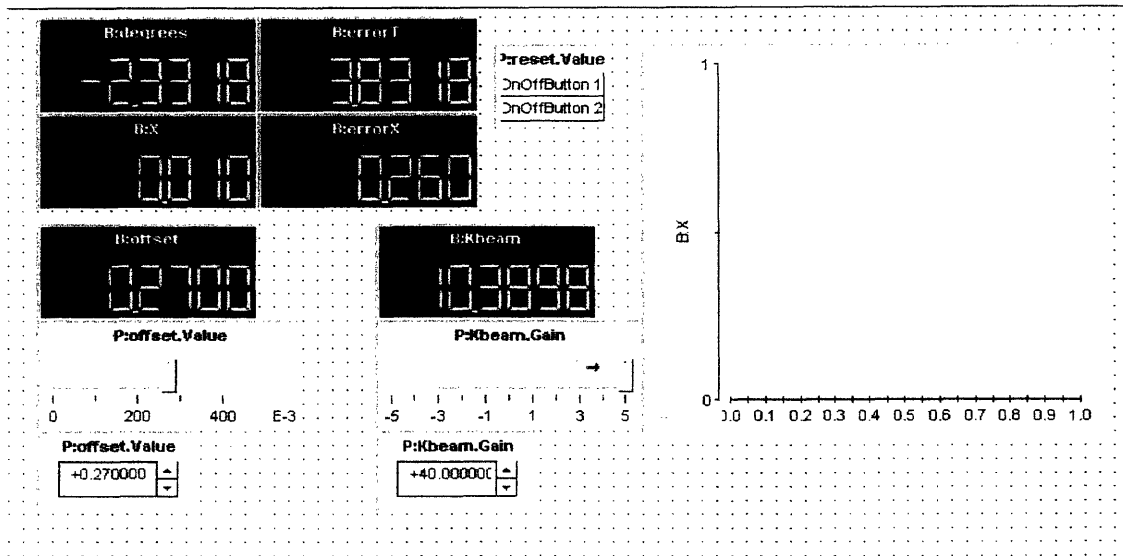ink block and Matlab script developed by Katherine Lilienkamp [9]. This dynamic analyzer provided a swept sine signal to drive an input and measure the output compared to an input designated anywhere along the loop. The analyzer then calculated a transfer function and graphed the Bode plot.

6.1 Motor

The motor was designed to perform at a high bandwidth and diminish error. The expected behavior is described by the transfer function in Equation 5.4. The step response of the ideal situation shown in Figure 5.4 and its Bode plot in Figure 5.5 can be compared to Figure 6.1 and Figure 6.2 respectively. The theoretical model and the physical plant closely match. Whereas the idealized bandwidth was 25 Hz, the real bandwidth was about 22 Hz. The damping also differed with the physical plant having more natural damping than expected. Despite the subtle differences, the plant was tuned well enough to resemble the designed model.
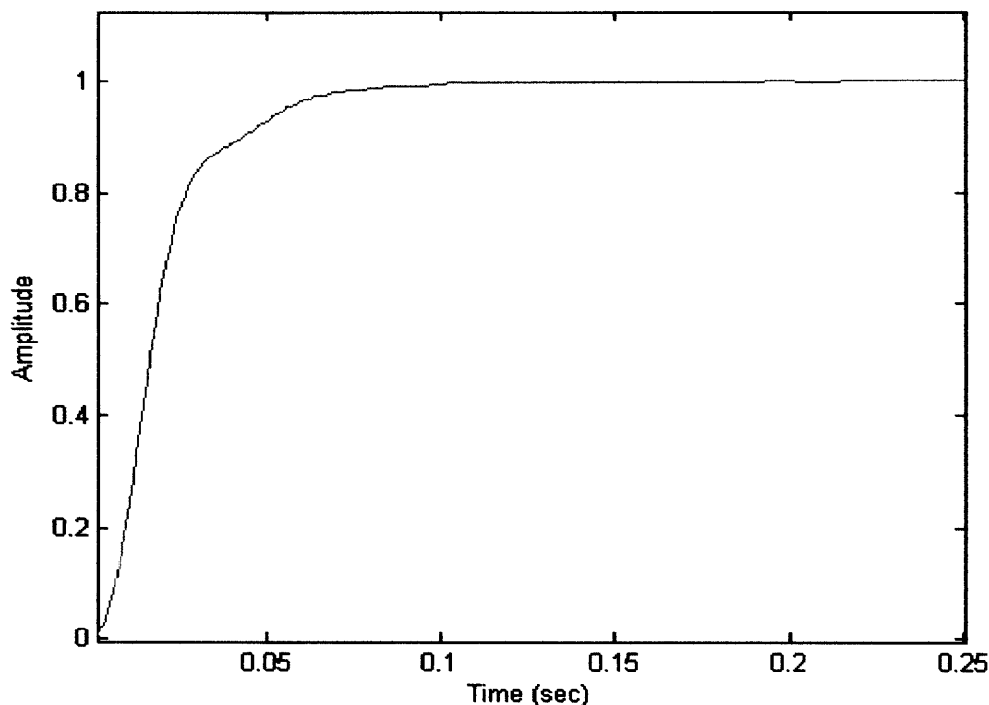
Figure 6.1. Actual Motor Step Response. The step response of the motor was measured by commanding a step in the motor alone and measuring the resulting transient in angular position.
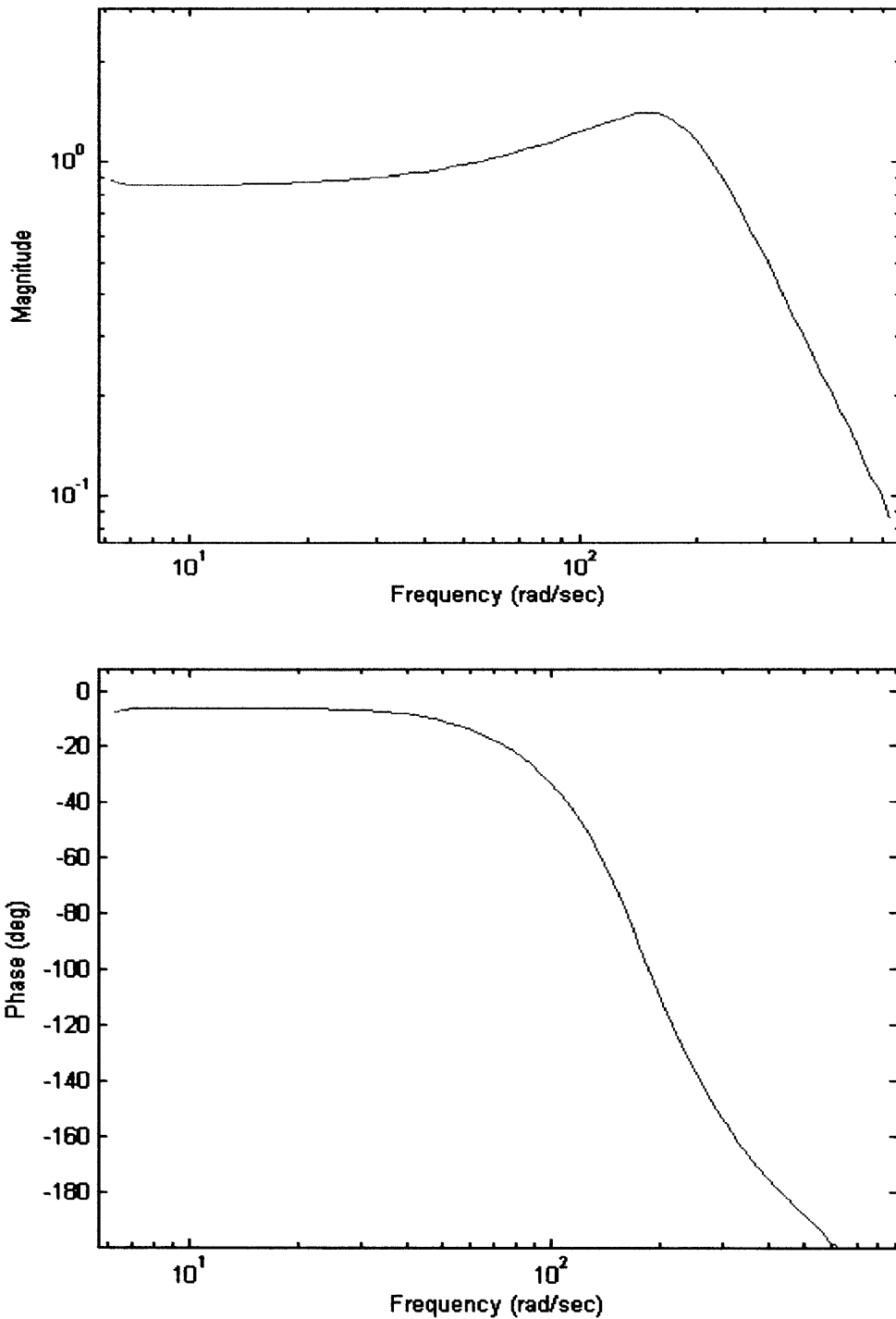
Figure 6.2. Measured Motor Bode Plot. The Bode plot was measured using a dynamic analyzer that calculated the transfer function and plotted the corresponding Bode plot.

6.2 Beam

The angle of the beam was not directly measured. Instead, the angle displacement of the motor, when attached to the beam, was measured. The Bode plot in Figure 6.3 shows how the motor angle in this coupled junction responded to varying frequencies. For low frequencies, the beam closely followed the motor. However, after passing the first resonance, anti-resonance occurred. At this frequency, excitation caused a small amplitude in the motor, but a large reaction in the beam. This physical plant feature limited the dynamic capabilities, although, the ball was not designed to operate faster than the first crossover frequency.
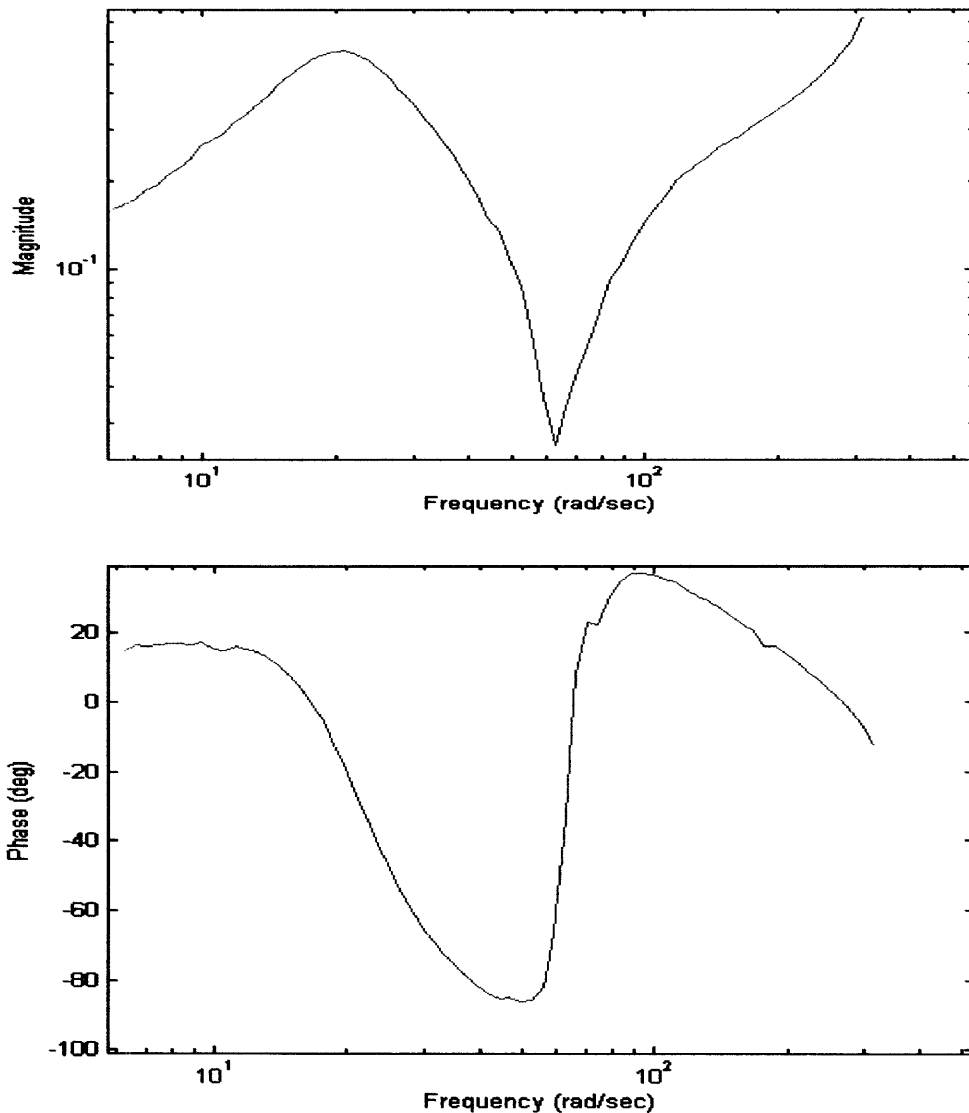
Figure 6.3. Measured Bode Plot of Motor and Beam. This Bode plot was generated for the closed loop performance of the motor when supporting the inertia of the beam. The coupling between the motor and the beam caused an anti-resonance to occur after the first resonance.

6.3 Ball

Having correctly closed the control loop of the motor, the closed loop of the ball was expected to perform as predicted and have the ball achieve the designed parameters. The system gains had to be adjusted to attain adequate stiffness and damping. Once satisfied with the adjustments, and once the ball was controlled at the center of the beam, a disturbance was applied to the ball. As expected, the beam rotated to force the ball back to its original position. If any oscillation was observed, the system was stable if the peak displacement of an oscillation was less than the previous oscillation. This test showed that the controller worked. Again, the system gain was adjusted to tune the oscillations out. Eventually, what resulted was a critically damped step response. A step command (Figure 6.4) could be ordered through the ControlDesk user interface. Essentially, the ball could be balanced at any position along the beam. For small step commands, the ball tracked the position quickly and without overshooting. For large step commands, the ball tended to either overshoot and oscillated several times before coming to rest, or to become unstable and lose system equilibrium. This defect can be attributed to the non-linearity in the system as well as the unreliability of the position sensor, which will be discussed in the next chapter. The non-linearity included the beam rotation angle dynamics, which was defined to be linear for small angles, and the contact of the ball on the beam. For the bigger step commands the control effort became large enough to command a significantly large beam rotation that initiated system instability.
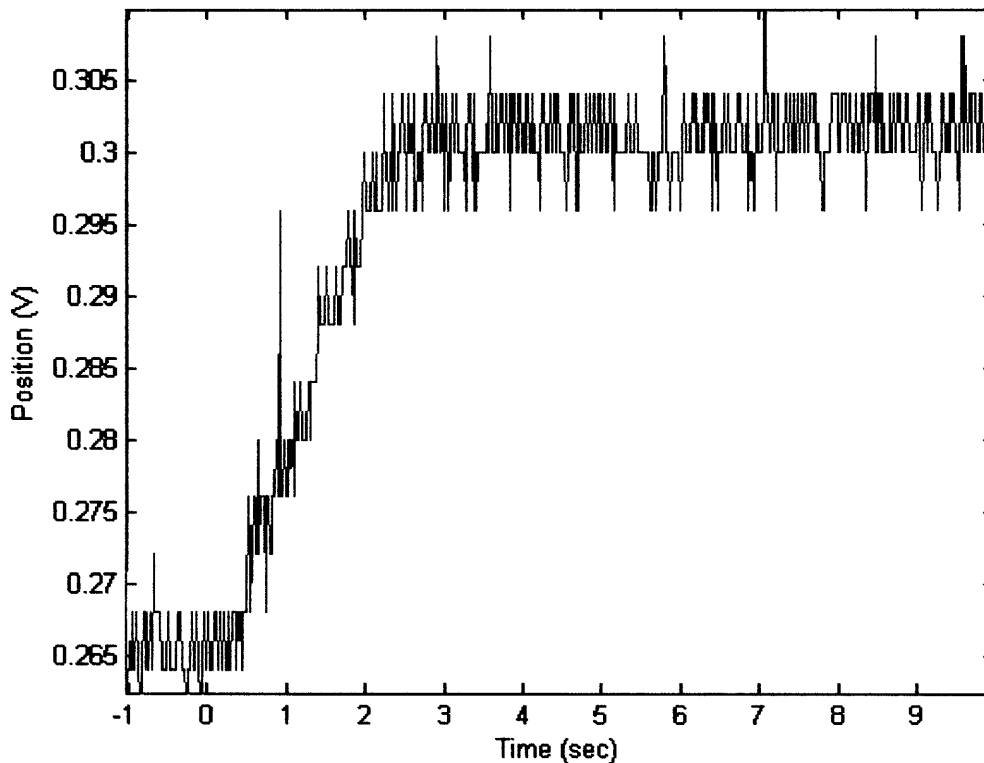

Figure 6.4. Measured Ball Step Command. For a small step command, the ball reached its new position without overshooting.

Chapter 7: Sensor Issues

The biggest difficulties encountered in this project were introduced by the unreliability of the ball position sensor. Because this sensor measured the system output, it was the most critical component of the apparatus. If the position of the ball was not exactly known, the position could not be precisely commanded. Noise that was introduced through this sensor severely paralyzed the performance of the overall system. With the linear potentiometer that was used in this set-up, the noise was a result of poor contact between the resistive element and the conductive ball. Signal dropout occurred intermittently as the ball rolled along the beam. For better signal transmission between the ball and the contact sensor, the materials should be more carefully chosen. Steel tends to oxidize easily and the oxide layer on the ball significantly increases the contact resistance. A beryllium-copper ball may be a better choice because the oxide of such a ball is also conductive.

7.1 Tested Ball Position Sensors

Several options were explored before settling on the final ball position sensor design. All the sensors tested were some variation of a linear potentiometer. A voltage source was conducted through one length of conductive rail while the other rail acted as a probe that picked off the voltage through the ball in the same manner as a voltage divider.

The first material used as a rail was a train track as per the set-up used by Bob Pease [4]. Two N-gauge model railroad track segments about two-feet long were mounted onto the beam. Current was driven through one rail to produce a voltage across the rail, while the other rail sensed the position as the ball came in contact with the two rails. The first problem with this set-up lay in the resistance of the railroad track. For a piece about two-feet long, the resistance of the N-gauge track was about 0.5 ohms. This meant that a large current was needed to produce any significant voltage. Even with 1 A of current producing 0.5 V, the resolution was poor, and the signal was noisy. High contact resistance between the ball and the rail also caused large signal dropouts.

The next iterations of the rail design were primarily intended to reduce the power requirements of the sensor. To meet this goal, the rail needed a higher resistance, which could be accomplished through having a smaller cross-sectional area or choosing a more resistive material. Two lengths of 1/64" steel welding rod were affixed to the beam in place of the train track and tested as a linear potentiometer sensor. The resistance across a two-foot length of rod was about 2 ohms. This reduced the power consumption, but the problem of poor contact resistance still remained. Just as with the train track, signal fallout occurred even after cleaning ball and rail surfaces.

Another rail sensor material tested was a conductive plastic. Conductive polyolefin, with a volume resistivity of about 3000 ohm/cm, was purchased from Westlake Plastics, and cut into 1/16" x 1" x 24" strips. The resistance across a length was about 150k ohms.

This element provided excellent resolution with minimal power consumption. However, the conductivity of this plastic was questionable. The surface of the plastic was susceptible to scratches that would substantially increase the contact resistance, and sufficient contact pressure was necessary for the ball to make good contact with the rails. Under dynamic conditions, the ball was not guaranteed to have this pressure and the signal often disappeared.

The final version of the sensor came from a packaged linear potentiometer with a two-foot stroke. The resistive elements of Novotechnik TL600 linear potentiometers were used as the senor for the ball position. The leads on which the wiper contacted were coated with a layer of conductive material. The resistance across the length of the element was about 20k ohms. Each element was positioned on the beam so as to create a cradle for the ball to roll along where the point of contact was within the resistive portion of the element.

Of the sensors tested, the resistive element was the most effective. The resolution was adequate and didn't require a high-power source. The contact was not quite so good, but less signal fallout occurred than in the other sensors. Occasionally, some locations on the rail registered a dead spot. This was caused by a spec of dirt or other foreign matter resting on the rail. This problem was fixed by thoroughly cleaning the rail before use. In addition, applying a low-pass filter reduced signal fallout by adding a 0.1 μF capacitor.

7.2 Alternate Ball Position Sensors

A linear potentiometer sensing technique was the only method tested, but other techniques are possible and might have had better results. Some ideas involved contact sensors, while others involved non-contact sensors. These ideas included wound nichrome wire, touch pads, acoustic transmission lines, ultrasonic transducers, and infrared (IR) sensors.

Nickel-chromium (nichrome) wire is a highly resistive metal that is often used in heating coils. Because of nichrome's high resistivity, it is an attractive option as a sensor since it would provide higher resolution and require less power than most metals of the same size. In other classical implementations of the ball-on-beam problem, nichrome wire was used [5]. Noise was a troublesome issue in these cases as well. However, if wound on a plain or threaded dowel, the nichrome wire exposes less contact surface due to the curvature around the dowel. Less contact surface means there will be higher contact pressure and better conductivity from the ball to the sensor. The incremental pits also limit the acceleration of the ball and make the ball easier to stop.

Touch pads that are commonly found on laptop computers and ATM touch screens primarily work in one of three ways: resistive, capacitive, or acoustic wave changes. All touch pads are constructed in two layers, one layer monitoring changes in signals which are read by a processor and the other interfacing with the world and accepting changes in resistance or capacitance. Capacitive touch pads, such as those in ATMs, have a top

layer that stores electrical charge. As a person's finger comes in contact with the glass, charge moves from the top layer to the person's finger. This location is measured by calculating the relative difference in charge from circuits at different locations of the screen. Resistive touch pads have a conductive and resistive metallic layer that is held apart. As pressure is applied, the two layers come in contact. A computer calculates the change in electric field and its coordinates. Assuming the ball has enough mass to apply enough pressure to a level touch pad, a feasible resistive touch pad beam sensor could be designed. In this case, the ball would not have to be conductive. For a capacitive touch pad, the ball would have to be conductive.

Based on the notion of the acoustic wave touch pad, an acoustic wave transmission line sensor could be designed to determine the position of the ball along the beam. In this design an actuator propagates a wave along some medium such as a metal rod and the delayed reception is measured to determine if a disturbance was felt at a particular point on the rod.

Another acoustic solution would be an ultrasonic range sensor. This transducer does not require a solid medium to propagate. However, this sensor registers any foreign object present in the proximity. Again, this sensor design does not need a conductive ball to generate a position signal.

Lastly, a series of infrared sensors could be used to reveal the position of the ball on the beam. Using this digital sensor, the resolution would depend on how closely together the sensors can be arranged. The ball need not be conductive for this sensor design to function properly. As the ball rolls past a sensor, the infrared beam is interrupted and the feedback signal is sent to the controller.

Compared to the simplicity of the linear potentiometer, any of the sensors mentioned in this section require a greater design effort, cost, and computation. Clearly, much more thought must occur to decide how to apply these sensing techniques. These designs will require more extensive hardware and electronics, which would increase the cost of the system. Along with affixing the sensor to the beam, the feedback signal(s) must also be processed to supply the controller with the discrete position of the ball. For the purpose of making kits available to students in feedback courses, the most cost-effective design is the analog linear potentiometer described in this thesis.

7.3 Alternate Motor Angle Position Sensors

As described in Section 4.2, the motor angle was sensed by an encoder using quadrature counting. The encoder attached to the back of the motor was the most readily available method to calculate the position of the motor and was therefore used. Although this method was quite satisfactory, other methods could have been implemented. Two solutions to this problem that are not digital are a rotary potentiometer and an accelerometer.

32

A rotary potentiometer has a thin piece of resistive material on the hub of its case through which a voltage is applied. As the shaft is rotated, a wiper moves along a resistive track. The signal carried from the wiper is used to calculate the position of the shaft along the rotary path. This measurement may add some resistance to the rotation of the motor shaft, but the potentiometer's reading is reliable.

The other solution to measuring the angle of the motor is to use an accelerometer, otherwise known as a gyro sensor. These devices detect the change in acceleration by measuring the change in electrical capacitance between two plates. These sensors tend to be less reliable for level measurements. The signal must be integrated twice and centered about an index point. This sensor is not DC-decoupled and introduces substantial noise into the signal.

Chapter 8: Future Work

Besides researching different sensors and determining which technique is most advantageous for this application, there are other possible areas of improvement. The mechanical design of the apparatus is an area that does not affect the performance of the system, but it should be noted that a relocation of the center of gravity and a decrease of overall dimensions could reduce material and cost. Two other main areas that could be redesigned are the controller and the transmission mechanism. The controller can be fine-tuned and even converted to analog control and the transmission mechanism can become more rigid or be eliminated.

8.1 Analog Control

The controller for this project was implemented in dSPACE using a Simulink model as mentioned in Section 5.3. The digital controller made implementation and adjustments simpler. However, an analog controller would have made the control interface more compact and easier to transport. Because the controllers are both lead controllers, the circuitry could have been either active, with op-amps, or passive with only resistors and capacitors. Figure 8.1 shows a sample controller circuit that could be used to implement a lead controller as in Equation 5.6.
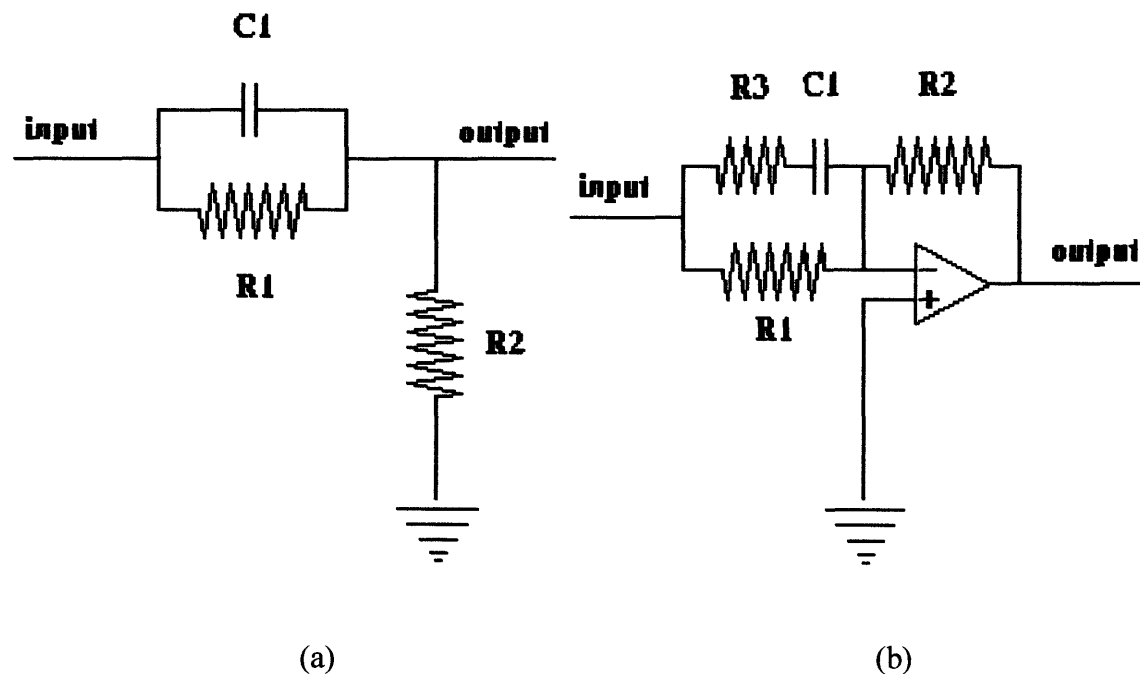
Figure 8.1. Analog Lead Controller. An analog lead controller could be implemented with either a passive circuit (a), or active circuit (b).

8.2 Transmission Redesign

Whereas the controller design can be adjusted to improve transient responses, the plant ultimately determines its limitations. Once the plant has been built, it can no longer be adjusted easily. A simple mechanical design can help improve the dynamic capability of the control system. To have a higher bandwidth and crossover frequency, either the inertia of the plant needs to decrease or the transmission mechanism needs to become stiffer. One way to make the transmission stiffer is to use a stiffer transmission belt than dental floss. Another way is to design stiffer flexures in the gear-reducing sector. The best way would be to completely remove the transmission and make the beam a direct drive. The initial reason for including a transmission was to provide mechanical advantage and enable the available motor to power the movements of the beam. Otherwise, as a direct drive, the given motor would not have been able to effectively manipulate the inertia of the beam. With a direct drive, the motor needs to be able to supply enough torque to support the mass of the ball at whatever distance away from the center that is desired. Using the current frame design, the motor and beam would also need additional support because the center of mass would be higher than its midpoint. Alternatively, the location of the beam could be lowered to move the center of gravity closer to the bottom of the structure.

Chapter 9: Conclusion

The ball-on-beam kit that was designed is simple, easy to assemble, and cost effective. It is also visually appealing and attractive as a decorative souvenir of a class project. Using this kit as a pedagogical instrument to teach feedback systems benefits both the instructor and the students. First, the kits are low cost, so there is not a big budget concern for the instructor. Second, this problem is interesting enough to capture the interest of most students. The ball-on-beam problem is a good opportunity to apply classical control.

Students in the feedback systems class in the electrical engineering department enjoyed designing controllers and the ball position sensor for the system. Most groups were successful in implementing their controller and sensor designs. There was a range of system successes, but all students learned valuable lessons.

The controller described in this thesis worked as designed. The main factor that troubled the controller was the poor quality of signal received from the ball position sensor. The noise, which was large for the first three sensors tested, saturated the amplifier because the derivative in the lead controller amplified the noise signal. Once the sensor was improved and the noise reduced, the controller worked as expected.

The most difficult part was indeed the ball position sensor design. This aspect of the project could be researched further. The ideas in Section 7.2 would be a starting point for possible sensor designs, and from those ideas, others would develop. In completing this project, it was often frustrating to realize that without a proper position measurement, control was impossible. A significant amount of time was spent testing different sensors and debugging them. After the initial mechanical and controller designs were done, attention was heavily focused on the design and success of the ball position sensor.

This project was a good opportunity to create hardware and implement a controller. The idiosyncrasies of real plants were revealed through variation and experimentation. These details were noted and can now be expected in similar cases. A sense of enthusiasm was developed and a passion to continue researching the area of controls was generated in the author.

Acknowledgments

Appendix A: Winchester Disk Drive Motor Specifications

These motor characteristics were converted to metric units from the English units used in the Litton Encoder Division data sheet for the Winchester Disk Drive Motor. The original specification sheet is on the subsequent page.

Constant	Value	Units	Description
k_t	3.885×10^{-2}	Nm/A	torque sensitivity
k_e	3.885×10^{-2}	V/rad/s	back EMF constant
R	3.7	ohms	armature resistance
k_m	2.02×10^{-2}	$Nm/\sqrt{W}$	motor constant
T_p	9.18×10^{-2}	Nm	peak torque
T_c	6.07×10^{-2}	Nm	continuous torque
J_r	1.2×10^{-5}	Nms^2	rotor inertia
B	4.45×10^{-4}	Nm/rad/s	viscous damping

1.0 DESCRIPTION: This specification defines an encoder to be coupled to a Limited Angle Brushless DC Motor in a 5¼ Winchester Disk Drive

The encoder is to provide three output signals. One output is Channel A; second is Channel B; and the third is an Index or Reference Pulse. Channels A and B exhibit a relationship such that A is a Sine function, while B performs the Cosine function.

The outputs from the Sine and the Cosine are analog and represent the actual resolution on the code disk.

Any reference of CW or CCW rotation in the following is assumed to be seen from the encoder side of the motor.

2.0 MECHANICAL CHARACTERISTICS:

  2.1 MOTOR/ENCODER DIMENSIONS   1.545" MAX (REF FIG 1) SHT 5

      2.1.1 MOTOR   1.006" MAX

      2.1.2 ENCODER   .539" MAX

      2.1.3 SHAFT DIAMETER (LOAD SIDE)   .2500 $^{+.0000"}_{-.0005"}$

      2.1.4 SHAFT LENGTH (LOAD SIDE)   .82 MAX

  2.2 COMM/HUB INERTIA $200\ (10^{-6})$ OZ-IN SEC^2 MAX

  2.3 RESOLUTION   1100 CYCLES/REV

      2.3.1 INDEX   1 PULSE/REV 5 CYCLES LONG

  2.4 SPEED   600 RPM MAX

  2.5 ACCELERATION   6000 RAD/SEC^2 MAX

3.0 MOTOR CHARACTERISTICS @20°C:

  3.1 EXCURSION ANGLE $^+_-60°$ 0

  3.2 TORQUE SENSITIVITY   5.5 OZ-IN/AMP   Kt

  3.3 BACK EMF CONSTANT   .0388 VOLTS/RADS/SEC   Ke

  3.4 RESISTANCE   3.7Ω   R

  3.5 MOTOR CONSTANT   2.86 OZ-IN/$\sqrt{WATTS}$ Km

  3.6 PEAK TORQUE   13 OZ-IN   Tp

  3.7 CONTINUOUS TORQUE   8.6 OZ-IN   Tc

  3.8 ROTOR INERTIA $1.7\ (10^{-3})$ OZ-IN-SEC^2 Jr

  3.9 VISCOUS DAMPING (ZERO IMPEDANCE)   .063 OZ-IN/RAD/SEC   D

References

[1] Product Information Sheet R2-1, Rotary Ball & Beam Experiment, Quanser Inc., Markham, ON, Canada.

[2] R. Hirsch, Shandor Motion Systems, "Ball on Beam Instructional System," Shandor Motion Systems, 1999.

[3] K. C. Craig, J. A. de Marchi, "Mechatronic System Design at Rensselaer," in 1995 International Conference on Recent Advances in Mechatronics, Istanbul, Turkey, August 14-16.

[4] R. A. Pease, "What's All This Ball-On-Beam-Balancing Stuff, Anyhow," Electronic Design Analog Applications, p. 50-52, November 20, 1995.

[5] G. J. Kenwood, "Modern control of the classic ball and beam problem," B.S. thesis, Massachusetts Institute of Technology, Cambridge, MA, 1982.

[6] C. Richard, A. M. Okamura, M. R. Cutkosky, "Getting a Feel for Dynamics: Using Haptic Interface Kits for Teaching Dynamics and Controls," 1997 ASME IMECE 6th Annual Symposium on Haptic Interfaces, Dallas, TX, Nov. 15-21.

[7] "Laboratory Assignment 4: Brushless Motor Control," lab handout for 2.737 Mechatronics, Department of Mechanical Engineering, Massachusetts Institute of Technology, Spring 1999.

[8] Gurley Precision Instruments, "Understanding Quadrature," 1998, http://www.gpi-encoders.com/Understanding_Quadrature.pdf.

[9] K. A. Lilienkamp, "A simulink-driven dynamic signal analyzer," B.S. thesis, Massachusetts Institute of Technology, Cambridge, MA, 1999.